PHYSICAL REVIEW E **100**, 010601(R) (2019)

Rapid Communications

Bose-Einstein-like condensation in scalar active matter with diffusivity edge

Ramin Golestanian[*]
Max Planck Institute for Dynamics and Self-Organization (MPIDS), 37077 Göttingen, Germany
and Rudolf Peierls Centre for Theoretical Physics, University of Oxford, Oxford OX1 3PU, United Kingdom

(Received 2 February 2019; revised manuscript received 17 April 2019; published 15 July 2019)

Due to their remarkable properties, systems that exhibit self-organization of their components resulting from intrinsic microscopic activity have been extensively studied in the last two decades. In a generic class of active matter, the interactions between the active components are represented via an effective density-dependent diffusivity in a mean-field single-particle description. Here, a class of scalar active matter is proposed by incorporating a diffusivity edge into the dynamics: when the local density of the system surpasses a critical threshold, the diffusivity vanishes. The effect of the diffusivity edge is studied under the influence of an external potential, which introduces the ability to control the behavior of the system by changing an effective temperature, which is defined in terms of the single-particle diffusivity and mobility. At a critical effective temperature, a system that is trapped by a harmonic potential is found to undergo a condensation transition, which manifests formal similarities to Bose-Einstein condensation.

DOI: 10.1103/PhysRevE.100.010601

Dense active matter provides an enthralling paradigm as its emergent properties are determined by competition between opposing tendencies that originate from both equilibrium and nonequilibrium processes [1,2]. In particular, the proximity of the active agents—through various nonequilibrium processes such as hydrodynamic interactions [3], chemical signaling [4–7], etc.—might lead to a collective enhancement of activity [8,9] and triggering of instabilities [10–12], whereas short-ranged physical interactions such as those arising from stickiness and excluded volume effects (and possibly some nonequilibrium processes as well) inhibit the collective activity [13–17], ultimately leading to the formation of globally ordered dense structures [18–20] or dynamic arrest [21,22]. In the absence of long-range orientational ordering, which can be caused by alignment interactions between polar agents in sufficiently dense systems [23,24], the activity of individual particles can be described by effective enhanced diffusion coefficients beyond the timescale of rotational diffusion [25]. In this regime, the system can be generically described using dynamical equations for the density field at the mean-field level. Here, we study such a description of scalar active matter with a generic density dependence in the diffusivity that incorporates a finite threshold: above a critical density the diffusivity vanishes. We demonstrate that the existence of this *diffusivity edge* leads to a dynamical phase transition that can be categorized as an analog of Bose-Einstein condensation (BEC) despite the system being classical and nonequilibrium in nature. The present work builds on the recent surge in the development of generalized thermodynamic descriptions for nonequilibrium active matter [26,27].

We formulate a mean-field description of the dynamics of the colloidal system described by an effective single-particle density field $\rho(\boldsymbol{r}, t)$ that satisfies a conservation law $\partial_t \rho + \nabla \cdot \boldsymbol{J} = 0$ where the flux is defined as $\boldsymbol{J} = -D(\rho)\nabla\rho + \rho\boldsymbol{v}$ in terms of an effective density-dependent diffusivity $D(\rho)$ and the drift velocity $\boldsymbol{v}$. Similar equations have been studied in the context of generalized nonlinear Fokker-Planck equations and their applications in biological problems [28,29]. We assume that the drift originates from an external potential $U(\boldsymbol{r})$ and involves a density-dependent mobility $M(\rho)$, namely, $\boldsymbol{v} = M(\rho)(-\nabla U)$. Using the single-particle diffusivity $D_{\rm s} = D(\rho \to 0)$ and the single-particle mobility $M_{\rm s} = M(\rho \to 0)$, we define an effective temperature $T_{\rm eff}$ that by construction satisfies the fluctuation-dissipation theorem (FDT), namely, $k_{\rm B}T_{\rm eff} \equiv D_{\rm s}/M_{\rm s}$, and define $\beta \equiv 1/(k_{\rm B}T_{\rm eff})$ for simplicity of notation. It is important to note that this definition of effective temperature is only meant as a symbolic representation of the measure of activity of the individual particles that can be used as a tuning parameter in our generalized thermodynamic description below. It has been shown that in the presence of external fields and orientational bias the single-particle activity cannot be represented by a single scalar effective temperature [30,31].

We incorporate a generic nonequilibrium character for the system by assuming a breakdown of FDT at finite densities, namely, $D(\rho)/M(\rho) \neq D_{\rm s}/M_{\rm s}$. We assume that this occurs due to density-dependent nonequilibrium effects, which could materialize as a result of collective inhibition as well as collective activation due to motility. Therefore, the diffusivity $D(\rho)$ and the mobility $M(\rho)$ will start from their single-particle values for dilute systems and can in general go up or down as the density is increased. To complete the formulation, we define a diffusivity edge at concentration $\rho_{\rm c}$ as follows: $D(\rho)/M(\rho) = 0$ for $\rho \geqslant \rho_{\rm c}$. We note that in this work we ignore nonlocal effects that arise from hydrodynamic interactions when FDT is broken [32] as well as long-range nonequilibrium interactions [12]. Note also that the external potential can also play the role of a diffusivity edge and

---

[*] ramin.golestanian@ds.mpg.de

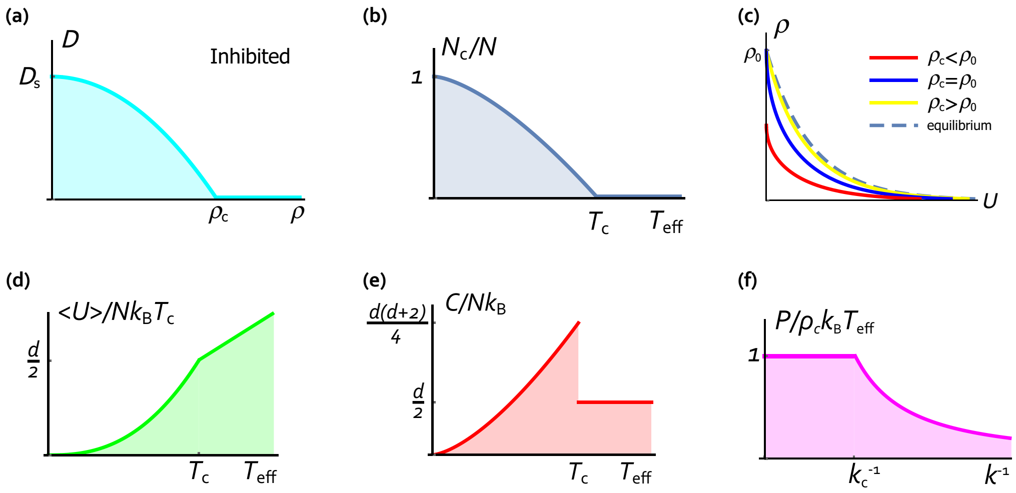

FIG. 1. The effect of inhibition in the presence of a diffusivity edge. (a) The density-dependent diffusivity for an inhibited system where the collective inhibition effects cause the diffusivity to decrease until it vanishes. (b) The fraction of particles in the Bose condensate as a function of the effective temperature near the critical transition temperature $T_{\rm c}$. (c) The stationary-state distribution for different values of $\rho_{\rm c}$ vs ρ_0. (d) The average internal energy for a d-dimensional system with a step function diffusivity profile. (e) The heat capacity of the system showing an overshoot and a discontinuity. (f) The pressure isotherm as calculated from changing the typical confinement size $\lambda = (2\pi k_{\rm B}T_{\rm eff}/k)^{1/2}$ through changing k^{-1}.

this can generate a competition with the contributions to the diffusivity edge that come from the interactions.

We then seek possible stationary states of the system as obtained by setting the net flux $\boldsymbol{J}/D_{\rm s} = -(D(\rho)/D_{\rm s})\nabla\rho - (M(\rho)/M_{\rm s})\rho\nabla\beta U$ to zero. This yields $\frac{d\beta U}{d\rho} = -\frac{M_{\rm s}D(\rho)}{D_{\rm s}M(\rho)\rho}$, and consequently

$$\beta U = -\int_{\rho_0}^{\rho}\frac{d\rho'}{\rho'}\,\frac{D(\rho')}{D_{\rm s}}\,\frac{M_{\rm s}}{M(\rho')}, \tag{1}$$

where ρ_0 is defined as the density at which energy is at its lowest value of zero (i.e., the ground state of the energy spectrum) that will correspond to the highest density in the spectrum (or profile if energy depends on position). The stationary distribution $\rho(U)$ can then be obtained by inverting Eq. (1). The energy can originate from gravity or an externally applied trapping potential, say by using holographic optical traps [2]. Note that henceforth, we are going to represent $M_{\rm s}D(\rho)/(D_{\rm s}M(\rho))$ as $D(\rho)/D_{\rm s}$ to keep the presentation simple.

The normalization condition for a total of N particles in d dimensions reads $N = \int d^d\boldsymbol{r}\,\rho(U(\boldsymbol{r})) = \int S_d r^{d-1}dr\,\rho(U(r))$ assuming that the potential is spherically symmetric, where $S_d = 2\pi^{d/2}/\Gamma(d/2)$ is the surface area of the unit sphere embedded in d dimensions. If $U(r)$ can be inverted (to a single-valued function), the normalization condition can be written as $N = \int_0^\infty dU\,g(U)\rho(U)$ where $g(U) \equiv S_d(r(U))^{d-1}\frac{dr}{dU}$ is the density of states. For example, a harmonic trap in the form of $U = \frac{1}{2}kr^2$ yields $g(U) = \frac{S_d}{2}(\frac{2}{k})^{d/2}U^{(d/2)-1}$. Since U is a monotonically decaying function of ρ, we can rewrite the normalization condition as follows:

$$N = \frac{k_{\rm B}T_{\rm eff}}{D_{\rm s}}\int_0^{\rho_0} d\rho\,D(\rho)\,g(U(\rho)) \qquad (\rho_0 < \rho_{\rm c}). \tag{2}$$

This condition gives $\rho_0(T_{\rm eff})$, which we expect to be a decreasing function of temperature. However, it only applies when $\rho_0 < \rho_{\rm c}$ as noted. This is because when $\rho_0 \geqslant \rho_{\rm c}$, the integrand in Eq. (2) vanishes identically and no longer contributes, which makes it impossible for the normalization to be satisfied. Therefore, the system develops a condensate with $N_{\rm c}$ particles at the ground state, and the normalization reads

$$N = N_{\rm c} + \frac{k_{\rm B}T_{\rm eff}}{D_{\rm s}}\int_0^{\rho_{\rm c}} d\rho\,D(\rho)\,g(U(\rho)) \qquad (\rho_0 \geqslant \rho_{\rm c}). \tag{3}$$

We can calculate the size of the condensate as a function of temperature below the transition temperature $T_{\rm c}$, which can be obtained by setting $\rho_0(T_{\rm c}) = \rho_{\rm c}$. When $T_{\rm eff} \leqslant T_{\rm c}$ (corresponding to $\rho_0 \geqslant \rho_{\rm c}$), Eq. (1) tells us that $\beta U(\rho) = u(\rho/\rho_{\rm c})$. Noting that $D(\rho) = D_{\rm s}\gamma(\rho/\rho_{\rm c})$ by definition, we can recast Eq. (3) into the form $N = N_{\rm c} + (k_{\rm B}T_{\rm eff})^{d/2}\frac{S_d}{2}(\frac{2}{k})^{d/2}\rho_{\rm c}\int_0^1 ds\,\gamma(s)(u(s))^{(d/2)-1}$. Noting that $T_{\rm c}$ corresponds to $N_{\rm c} = 0$, this calculation yields the fraction of particles in the condensate as

$$\frac{N_{\rm c}}{N} = 1 - \left(\frac{T_{\rm eff}}{T_{\rm c}}\right)^{d/2}. \tag{4}$$

This result is plotted in Fig. 1(b). Below, we will examine the behavior of systems that undergo such a condensation transition more concretely, using a number of specific cases.

Consider a situation where inhibition causes the effective diffusivity in this mean-field description to monotonically decrease as a function of density, until it vanishes at $\rho = \rho_{\rm c}$. Figure 1(a) shows the density-dependent diffusivity, and the resulting stationary distribution $\rho(U)$ is presented in Fig. 1(c). For $\rho_0 \ll \rho_{\rm c}$ the distribution approaches a Boltzmann weight $\rho_0 e^{-\beta U}$ while increasing ρ_0 with respect to $\rho_{\rm c}$ leads to progressively faster-than-exponential decay, until the slope of the distribution diverges at $U = 0$ for $\rho_0 = \rho_{\rm c}$, which is the onset of condensation. For $\rho_0 > \rho_{\rm c}$, the slope at $U = 0$ continues to diverge, while the asymptotic value $\rho(U \to 0^+) = \rho_{\rm c}$ will be systematically smaller than ρ_0. This signals the presence of a condensate at $U = 0$, which populates N_c particles as determined by Eqs. (3) and (4).

To better illustrate the properties of the condensation transition let us consider a step function profile for diffusivity, namely, $D(\rho < \rho_\mathrm{c}) = D_\mathrm{s}$ and $D(\rho > \rho_\mathrm{c}) = 0$. Then, for the stationary distribution ρ we find $\rho_0 e^{-\beta U}$ for $\rho_0 < \rho_\mathrm{c}$ and $\rho_\mathrm{c} e^{-\beta U}$ for $\rho_0 \geqslant \rho_\mathrm{c}$. Using this explicit form, we can use the normalization condition Eq. (2) to obtain the value of ρ_0, which for the harmonic potential yields $\rho_0 = N(2\pi k_\mathrm{B} T_\mathrm{eff}/k)^{-d/2}$. Using this, we can find the transition temperature as $T_\mathrm{c} = \frac{k}{2\pi k_\mathrm{B}}(N/\rho_\mathrm{c})^{2/d}$ by setting $\rho_0(T_\mathrm{c}) = \rho_\mathrm{c}$. We can also calculate the average energy of the system as $\langle U \rangle = \int_0^\infty dU\, g(U) U \rho(U)$. This yields

$$\langle U \rangle = \begin{cases} \frac{d}{2} N k_\mathrm{B} T_\mathrm{eff}, & \text{for } \rho_0 < \rho_\mathrm{c} \\ \frac{d}{2}\left(\frac{2\pi}{k}\right)^{d/2} \rho_\mathrm{c} (k_\mathrm{B} T_\mathrm{eff})^{(d/2)+1}, & \text{for } \rho_0 \geqslant \rho_\mathrm{c}, \end{cases} \tag{5}$$

which can be rewritten as

$$\langle U \rangle = \frac{d}{2} N k_\mathrm{B} T_\mathrm{eff} \begin{cases} \left(\frac{T_\mathrm{eff}}{T_\mathrm{c}}\right)^{d/2}, & \text{for } T_\mathrm{eff} \leqslant T_\mathrm{c} \\ 1, & \text{for } T_\mathrm{eff} > T_\mathrm{c}. \end{cases} \tag{6}$$

This result is plotted in Fig. 1(d). Consequently, we obtain the following expression for the heat capacity of the system:

$$C = \frac{d\langle U \rangle}{dT_\mathrm{eff}} = \frac{d}{2} N k_\mathrm{B} \begin{cases} \left(\frac{d}{2}+1\right)\left(\frac{T_\mathrm{eff}}{T_\mathrm{c}}\right)^{d/2}, & \text{for } T_\mathrm{eff} \leqslant T_\mathrm{c} \\ 1, & \text{for } T_\mathrm{eff} > T_\mathrm{c}, \end{cases} \tag{7}$$

which is plotted in Fig. 1(e). We can construct other generalized thermodynamic functions. We can define entropy via $dS = dU/T_\mathrm{eff}$, and find

$$S = \begin{cases} \left(\frac{d}{2}+1\right) N k_\mathrm{B} \left(\frac{T_\mathrm{eff}}{T_\mathrm{c}}\right)^{d/2}, & \text{for } T_\mathrm{eff} \leqslant T_\mathrm{c} \\ \left(\frac{d}{2}+1\right) N k_\mathrm{B} + \frac{d}{2} N k_\mathrm{B} \ln\left(\frac{T_\mathrm{eff}}{T_\mathrm{c}}\right), & \text{for } T_\mathrm{eff} > T_\mathrm{c}. \end{cases} \tag{8}$$

The expression for $T_\mathrm{eff} \leqslant T_\mathrm{c}$ satisfies the Nernst rule and can be written as $S(T_\mathrm{eff} \leqslant T_\mathrm{c}) = (\frac{d}{2}+1)(N - N_\mathrm{c}) k_\mathrm{B}$, which reveals that condensed particles carry zero entropy and that there is a latent heat associated with the transition in a coexistence. Although the system does not have a fixed volume, we can calculate the average system size as $\lambda = (2\pi k_\mathrm{B} T_\mathrm{eff}/k)^{1/2}$ and define an effective volume $V = \lambda^d$. It is possible to define a Helmholtz free energy $F = U - T_\mathrm{eff} S$ and use it to calculate pressure via $P = -(\frac{\partial U}{\partial V})_{T_\mathrm{eff}} = (\frac{2}{d})\frac{k}{V}\frac{\partial F}{\partial k}$. For isotherms, the transition happens at a critical stiffness $k_\mathrm{c} = \frac{2\pi k_\mathrm{B} T_\mathrm{eff}}{(N/\rho_\mathrm{c})^{2/d}}$. We find

$$P = \begin{cases} \rho_\mathrm{c} k_\mathrm{B} T_\mathrm{eff}, & \text{for } k^{-1} \leqslant k_\mathrm{c}^{-1} \\ \frac{N/(2\pi)^{d/2}}{(k_\mathrm{B} T_\mathrm{eff})^{d/2-1}} \frac{1}{k^{-d/2}}, & \text{for } k^{-1} > k_\mathrm{c}^{-1}, \end{cases} \tag{9}$$

which is plotted in Fig. 1(f). This result can also be found through a mechanical definition of pressure, by integrating average force over a bounding surface area [33]. Eliminating the effective temperature, we find that the critical point for the pressure isotherms always lie on the curve defined by $P_\mathrm{c} = \frac{1}{2\pi} N^{2/d} \rho_\mathrm{c}^{1-2/d}/k_\mathrm{c}^{-1}$. The isothermal compressibility can be defined via $\kappa_{T_\mathrm{eff}}^{-1} = -V(\frac{\partial P}{\partial V})_{T_\mathrm{eff}}$. We observe that κ_{T_eff} diverges for $k^{-1} \leqslant k_\mathrm{c}^{-1}$. Equations (4), (7)–(9) highlight a strong analogy to the thermodynamics of BEC [34–36]. There are also subtle differences. The discontinuity in the heat capacity curve, which does not exist for dimensions less than five in normal BEC [35], is a consequence of the discrete jump in diffusivity at ρ_c. For a normal BEC, the divergence of the isothermal incompressibility is connected to the existence of off-diagonal–long-range order (ODLRO) via the FDT that relates density correlations to the compressibility. We do not have access to the density correlations at this level of description in our theory, since it is constructed at the mean-field level. It will be interesting to generalize the present framework to account for fluctuations and investigate the question of the existence of ODLRO in our model.

We next consider a $D(\rho)$ profile that contains collective activation at intermediate densities before the inhibition at higher level of crowding gives rise to a diffusivity edge, as shown in Fig. 2(a). This type of enhancement of activity has been observed to arise from hydrodynamic interactions [8,9] and can arise also from alignment interactions—below the onset of flocking, so that the system can still be described by a scalar order parameter. In this case, the stationary distribution that is shown in Fig. 2(b) shows a tendency for the particles to occupy higher energy states more than the equilibrium case, while the formation of the Bose condensate happens by following the same stages as in the inhibited case, namely, divergence of the slope of $\rho(U)$ at $U = 0$ when $\rho_0 = \rho_\mathrm{c}$ and the subsequent depletion that is accompanied by the formation of the condensate at the ground state.

To further examine the effect of activity, we consider a piecewise diffusivity profile

$$D(\rho) = \begin{cases} D_\mathrm{s}, & \text{for } 0 \leqslant \rho < \rho_\mathrm{a} \\ D_\mathrm{a}, & \text{for } \rho_\mathrm{a} \leqslant \rho < \rho_\mathrm{c} \\ 0, & \text{for } \rho_\mathrm{c} \leqslant \rho, \end{cases} \tag{10}$$

where D_a is the diffusivity in the activated region. Let us define $\alpha \equiv D_\mathrm{a}/D_\mathrm{s}$ as the measure of activation. The behavior of the system will depend on how the ground-state density ρ_0 compares with the density scales ρ_a and ρ_c. The different categories are discussed below.

(a) Low-density regime $\rho_0 < \rho_\mathrm{a}$. The stationary solution in this regime is found as the Boltzmann weight $\rho_0 e^{-\beta U}$ with $\rho_0 = N(2\pi k_\mathrm{B} T_\mathrm{eff}/k)^{-d/2}$ and the average energy given as $\langle U \rangle = \frac{d}{2} N k_\mathrm{B} T_\mathrm{eff}$, which yields $C = \frac{d}{2} N k_\mathrm{B}$. Setting $\rho_0 = \rho_\mathrm{a}$, we find the transition temperature $T_\mathrm{a} = \frac{k}{2\pi k_\mathrm{B}}(N/\rho_\mathrm{a})^{2/d}$ below which the system will start to be influenced by the activation. The dilute regime corresponds to $T_\mathrm{eff} > T_\mathrm{a}$.

(b) Intermediate-density regime $\rho_\mathrm{a} \leqslant \rho_0 < \rho_\mathrm{c}$. In this range of densities, which corresponds to $T_\mathrm{eff} \leqslant T_\mathrm{a}$, the stationary solution is found as follows:

$$\rho(U) = \begin{cases} \rho_\mathrm{a}(\rho_0/\rho_\mathrm{a})^{\alpha} e^{-\beta U}, & \text{for } \rho < \rho_\mathrm{a} \\ \rho_0\, e^{-\beta U/\alpha}, & \text{for } \rho_\mathrm{a} \leqslant \rho < \rho_0, \end{cases} \tag{11}$$

which resembles a distribution with two different temperatures for different ranges of energy. In this regime, we obtain the particle number normalization condition as

$$N = \frac{\rho_\mathrm{a}(2\pi/k)^{d/2}}{\Gamma(d/2)} (k_\mathrm{B} T_\mathrm{eff})^{d/2} H_{d/2}\left(\alpha, \ln\frac{\rho_0}{\rho_\mathrm{a}}\right), \tag{12}$$

and the average internal energy content as

$$\langle U \rangle = \frac{\rho_\mathrm{a}(2\pi/k)^{d/2}}{\Gamma(d/2)} (k_\mathrm{B} T_\mathrm{eff})^{(d/2)+1} H_{(d/2)+1}\left(\alpha, \ln\frac{\rho_0}{\rho_\mathrm{a}}\right), \tag{13}$$

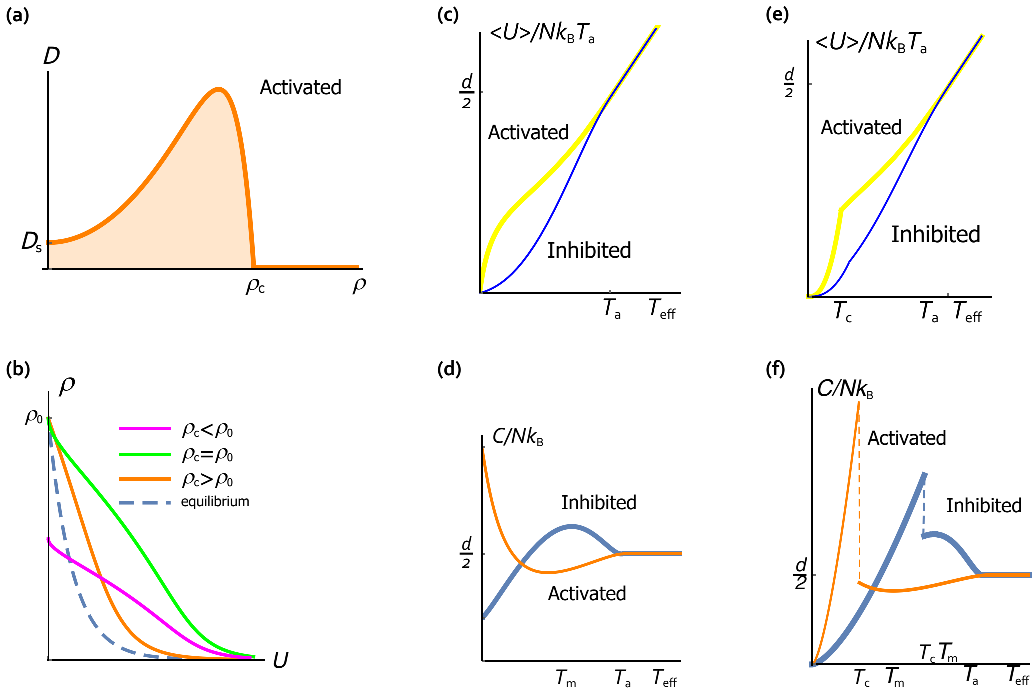

FIG. 2. The effect of activation in the presence a diffusivity edge. (a) The density-dependent diffusivity for an activated system where motility causes the diffusivity to increase initially until it starts to rapidly decrease due to inhibition and finally vanishes. (b) The resulting stationary-state distribution for different values of ρ_c vs ρ_0. (c) The average internal energy for a d-dimensional system as a function of temperature near the activity temperature T_a, for $\rho_c \to \infty$ (corresponding to $T_c \to 0$). The activated case corresponds to $\alpha > 1$ and the inhibited case corresponds to $\alpha < 1$. (d) The heat capacity of the system showing a dip for the activated case and an overshoot for the inhibited case, at an intermediate temperature $T_m < T_a$, for $\rho_c \to \infty$ (corresponding to $T_c \to 0$). The intercept at $T_{eff} = 0$ is equal to $\alpha d/2$. (e) The average internal energy for finite ρ_c, where a BEC appears at $T_{eff} < T_c$. (f) The heat capacity for the case with finite ρ_c. The plot shows an example where $T_c < T_m$. It is also possible to have the condensation before the temperature reaches the maximum or minimum.

in terms of the function $H_z(\alpha, p) \equiv e^p \alpha^z (\Gamma(z) - \Gamma(z, p)) + e^{p\alpha}\Gamma(z, \alpha p)$, where $\Gamma(z, p) = \int_p^\infty dx\, x^{z-1} e^{-x}$ is the upper incomplete gamma function. From the expression for average energy, we can calculate the heat capacity as follows:

$$\frac{C}{Nk_B} = \left(\frac{d}{2}+1\right)\frac{H_{(d/2)+1}\left(\alpha, \ln\frac{\rho_0}{\rho_a}\right)}{H_{(d/2)}\left(\alpha, \ln\frac{\rho_0}{\rho_a}\right)} - \left(\frac{d}{2}\right)\frac{H_{(d/2)+1}\left(\alpha, \ln\frac{\rho_0}{\rho_a}\right) + (\alpha-1)\left(\frac{\rho_0}{\rho_a}\right)^\alpha \Gamma\left(\frac{d}{2}+1, \alpha \ln\frac{\rho_0}{\rho_a}\right)}{H_{d/2}\left(\alpha, \ln\frac{\rho_0}{\rho_a}\right) + (\alpha-1)\left(\frac{\rho_0}{\rho_a}\right)^\alpha \Gamma\left(\frac{d}{2}, \alpha \ln\frac{\rho_0}{\rho_a}\right)}. \tag{14}$$

The average internal energy [shown in Fig. 2(c)] starts with a negative curvature for activated particles ($\alpha > 1$) and a positive curvature for inhibited particles ($\alpha < 1$). The slope of this curve corresponds to the heat capacity, which is shown in Fig. 2(d). It starts from $\alpha d/2$ (in units of Nk_B) at small effective temperatures and goes through a ripple before asymptotically approaching $d/2$ at sufficiently large effective temperatures. These results are valid at all effective temperatures (or densities) when $\rho_c \to \infty$.

(c) High-density regime $\rho_c \leqslant \rho_0$. For finite ρ_c there exists a regime at which the condensation happens when the density surpasses ρ_c. The stationary distribution in this case, which corresponds to $T_{eff} \leqslant T_c < T_a$, is given as

$$\rho(U) = \begin{cases} \rho_a(\rho_c/\rho_a)^\alpha e^{-\beta U}, & \text{for } \rho < \rho_a \\ \rho_c e^{-\beta U/\alpha}, & \text{for } \rho_a \leqslant \rho < \rho_c \\ \text{condensate}, & \text{for } \rho_c \leqslant \rho < \rho_0, \end{cases} \tag{15}$$

using which we can calculate the average internal energy as

$$\langle U \rangle = N \frac{H_{(d/2)+1}\left(\alpha, \ln\frac{\rho_c}{\rho_a}\right)}{H_{d/2}\left(\alpha, \ln\frac{\rho_c}{\rho_a}\right)} \left(\frac{T_{eff}}{T_c}\right)^{d/2} k_B T_{eff}, \tag{16}$$

and the heat capacity of the system as

$$C = Nk_B\left(\frac{d}{2}+1\right)\frac{H_{(d/2)+1}\left(\alpha, \ln\frac{\rho_c}{\rho_a}\right)}{H_{d/2}\left(\alpha, \ln\frac{\rho_c}{\rho_a}\right)}\left(\frac{T_{eff}}{T_c}\right)^{d/2}. \tag{17}$$

The corresponding plots of energy and heat capacity in this case are given in Figs. 2(e) and 2(f), respectively, where the system develops the condensate at $T_{eff} \leqslant T_c$, with the resulting characteristic discontinuity in the heat capacity.

(d) Relation to the quantum Bose gas. It is instructive to make the connection between the present model and the quantum statistics of bosons. The Bose distribution $\rho(U) = \rho_Q/(e^{\beta(U-\mu)} - 1)$ (where $\rho_Q = 1/\lambda_{dB}^d$ is the so-called

quantum concentration with λ_{dB} being the thermal de Broglie wavelength, and μ is the chemical potential) can be rewritten in the form of $\frac{d\beta U}{d\rho} = -\frac{D(\rho)}{D_{\mathrm{s}}\rho}$, which yields $\frac{D(\rho)}{D_{\mathrm{s}}} = \frac{1}{1+\rho/\rho_Q}$. This shows that for densities higher than the quantum concentration the system will effectively experience an inhibited diffusivity in the language of our description. The fact that a smooth decay that is not cut off by a diffusivity edge leads to BEC is due to the divergence of $\rho(U)$ as $U \to 0$ for bosons, which contrasts from our model where a finite maximum density of ρ_0 is assumed. We also note that the nature of the condensate in BEC is determined by the quantum mechanical characteristics of the system: it is described by a complex order parameter representing the macroscopic wave function and a broken U(1) gauge symmetry, unlike our classical nonequilibrium system.

We have thus shown that the existence of a diffusivity edge leads to the formation of a condensate, through a transition that has formal similarities to Bose-Einstein condensation. An example of active matter with a diffusivity edge that has been recently found in a system of magnetic bacteria in shear flow [37,38] will be presented elsewhere [39]. Our work has similarities with the formulation that is used to describe motility-induced phase separation (MIPS), with the key difference that the instability in MIPS is triggered by the effective diffusivity changing sign thereby promoting the formation of a dense cluster beyond a threshold density [13]. Enforcing the diffusivity edge preempts that instability and gives rise to a new behavior with formal similarities to BEC. We also note that in quantum mechanics we are limited to very specific forms of BEC, as the kinetic energy of bosonic particles can adopt only a limited number of forms; e.g., $p^2/2m$ for nonrelativistic massive bosons in dilute gases. Our formulation allows us to explore countless new types of BEC by designing appropriate forms of external trapping potential.

I would like to acknowledge helpful discussions with Benoît Mahault.

---

[1] M. C. Marchetti, J. F. Joanny, S. Ramaswamy, T. B. Liverpool, J. Prost, M. Rao, and R. A. Simha, Hydrodynamics of soft active matter, Rev. Mod. Phys. **85**, 1143 (2013).

[2] C. Bechinger, R. D. Leonardo, H. Löwen, C. Reichhardt, G. Volpe, and G. Volpe, Active particles in complex and crowded environments, Rev. Mod. Phys. **88**, 045006 (2016).

[3] J. Elgeti, R. G. Winkler, and G. Gompper, Physics of microswimmers—single particle motion and collective behavior: A review, Rep. Prog. Phys. **78**, 056601 (2015).

[4] E. F. Keller and L. A. Segel, Model for chemotaxis, J. Theor. Biol. **30**, 225 (1971).

[5] G. H. Wadhams and J. P. Armitage, Making sense of it all: Bacterial chemotaxis, Nat. Rev. Mol. Cell Biol. **5**, 1024 (2004).

[6] J. Taktikos, V. Zaburdaev, and H. Stark, Collective dynamics of model microorganisms with chemotactic signaling, Phys. Rev. E **85**, 051901 (2012).

[7] S. Saha, R. Golestanian, and S. Ramaswamy, Clusters, asters, and collective oscillations in chemotactic colloids, Phys. Rev. E **89**, 062316 (2014).

[8] A. Sokolov, I. S. Aranson, J. O. Kessler, and R. E. Goldstein, Concentration Dependence of the Collective Dynamics of Swimming Bacteria, Phys. Rev. Lett. **98**, 158102 (2007).

[9] T. Ishikawa, N. Yoshida, H. Ueno, M. Wiedeman, Y. Imai, and T. Yamaguchi, Energy Transport in a Concentrated Suspension of Bacteria, Phys. Rev. Lett. **107**, 028102 (2011).

[10] R. A. Simha and S. Ramaswamy, Hydrodynamic Fluctuations and Instabilities in Ordered Suspensions of Self-Propelled Particles, Phys. Rev. Lett. **89**, 058101 (2002).

[11] D. Saintillan and M. J. Shelley, Instabilities and Pattern Formation in Active Particle Suspensions: Kinetic Theory and Continuum Simulations, Phys. Rev. Lett. **100**, 178103 (2008).

[12] R. Golestanian, Collective Behavior of Thermally Active Colloids, Phys. Rev. Lett. **108**, 038303 (2012).

[13] M. E. Cates and J. Tailleur, Motility-induced phase separation, Annu. Rev. Condens. Matter Phys. **6**, 219 (2015).

[14] S. Henkes, Y. Fily, and M. C. Marchetti, Active jamming: Self-propelled soft particles at high density, Phys. Rev. E **84**, 040301(R) (2011).

[15] G. S. Redner, M. F. Hagan, and A. Baskaran, Structure and Dynamics of a Phase-Separating Active Colloidal Fluid, Phys. Rev. Lett. **110**, 055701 (2013).

[16] I. Buttinoni, J. Bialké, F. Kümmel, H. Löwen, C. Bechinger, and T. Speck, Dynamical Clustering and Phase Separation in Suspensions of Self-Propelled Colloidal Particles, Phys. Rev. Lett. **110**, 238301 (2013).

[17] R. Soto and R. Golestanian, Run-and-tumble dynamics in a crowded environment: Persistent exclusion process for swimmers, Phys. Rev. E **89**, 012706 (2014).

[18] J. Blaschke, M. Maurer, K. Menon, A. Zöttl, and H. Stark, Phase separation and coexistence of hydrodynamically interacting microswimmers, Soft Matter **12**, 9821 (2016).

[19] P. Digregorio, D. Levis, A. Suma, L. F. Cugliandolo, G. Gonnella, and I. Pagonabarraga, Full Phase Diagram of Active Brownian Disks: From Melting to Motility-Induced Phase Separation, Phys. Rev. Lett. **121**, 098003 (2018).

[20] C. A. Velasco, M. Abkenar, G. Gompper, and T. Auth, Collective behavior of self-propelled rods with quorum sensing, Phys. Rev. E **98**, 022605 (2018).

[21] P. J. Lu, E. Zaccarelli, F. Ciulla, A. B. Schofield, F. Sciortino, and D. A. Weitz, Gelation of particles with short-range attraction, Nature (London) **453**, 499 (2008).

[22] A. Cavagna, Supercooled liquids for pedestrians, Phys. Rep. **476**, 51 (2009).

[23] J. Toner and Y. Tu, Flocks, herds, and schools: A quantitative theory of flocking, Phys. Rev. E **58**, 4828 (1998).

[24] G. Grégoire and H. Chaté, Onset of Collective and Cohesive Motion, Phys. Rev. Lett. **92**, 025702 (2004).

[25] J. R. Howse, R. A. L. Jones, A. J. Ryan, T. Gough, R. Vafabakhsh, and R. Golestanian, Self-Motile Colloidal Particles: From Directed Propulsion to Random Walk, Phys. Rev. Lett. **99**, 048102 (2007).

[26] A. P. Solon, Y. Fily, A. Baskaran, M. E. Cates, Y. Kafri, M. Kardar, and J. Tailleur, Pressure is not a state function for generic active fluids, Nat. Phys. **11**, 673 (2015).

[27] A. Y. Grosberg and J.-F. Joanny, Nonequilibrium statistical mechanics of mixtures of particles in contact with different thermostats, Phys. Rev. E **92**, 032118 (2015).

[28] P. H. Chavanis, Nonlinear mean field Fokker-Planck equations. Application to the chemotaxis of biological populations, Eur. Phys. J. B **62**, 179 (2008).

[29] P.-H. Chavanis, Generalized stochastic Fokker-Planck equations, Entropy **17**, 3205 (2015).

[30] J. Tailleur and M. E. Cates, Sedimentation, trapping, and rectification of dilute bacteria, Europhys. Lett. **86**, 60002 (2009).

[31] C. Maggi, M. Paoluzzi, N. Pellicciotta, A. Lepore, L. Angelani, and R. D. Leonardo, Generalized Energy Equipartition in Harmonic Oscillators Driven by Active Baths, Phys. Rev. Lett. **113**, 238303 (2014).

[32] R. Golestanian and A. Ajdari, Tracer diffusivity in a time- or space-dependent temperature field, Europhys. Lett. **59**, 800 (2002).

[33] B. Mahault and R. Golestanian (unpublished).

[34] F. London, On the Bose-Einstein condensation, Phys. Rev. **54**, 947 (1938).

[35] R. M. Ziff, G. E. Uhlenbeck, and M. Kac, The ideal Bose-Einstein gas, revisited, Phys. Rep. **32**, 169 (1977).

[36] M. Kardar, *Statistical Physics of Particles* (Cambridge University Press, Cambridge, UK, 2007).

[37] N. Waisbord, C. T. Lefèvre, L. Bocquet, C. Ybert, and C. Cottin-Bizonne, Destabilization of a flow focused suspension of magnetotactic bacteria, Phys. Rev. Fluids **1**, 053203 (2016).

[38] F. Meng, D. Matsunaga, and R. Golestanian, Clustering of Magnetic Swimmers in a Poiseuille Flow, Phys. Rev. Lett. **120**, 188101 (2018).

[39] F. Meng, D. Matsunaga, J. M. Yeomans, and R. Golestanian (unpublished).